Journal of Civil Engineering and Construction Technology Vol. 3(11), pp. 291-301, December 2012
Available online at http://www.academicjournals.org/JCECT
DOI: 10.5897/JCECT12.043
ISSN 2141-2634 ©2012 Academic Journals

Full Length Research Paper

Hydration characteristics of cement pastes incorporating electric arc-furnace slag

S. O. Nwaubani[1]* and T. Z. Muntasser[2]

[1]Department of Built Environment, Anglia Ruskin University, Cambridge and Chelmsford, CM1 1SQ, Essex, UK.
[2]Department of Civil Engineering, University of Surrey, Guildford, GU2 9HX, Surrey, UK.

Accepted 22 October, 2012

This paper presents the results of a comparative study of the hydration characteristics of cement pastes incorporating steel slag or ground granulated blastfurnace slag (GGBS) as substitutes for ordinary Portland cement (OPC). The study looked at the physical and chemical characteristics of the starting materials. Various cementitious paste mixes were manufactured and cured under two separate curing regimes and a combination of thermogravimetric and X-Ray diffraction analysis used to identify the hydration products formed during the investigation. The study established that the partial replacement of OPC with Electric Arc-Furnace steel slag or GGBS leads to a slow rate of formation of hydration products at early ages. However, at later ages, mixtures containing GGBS and waste slag produced more hydration products than the control OPC mix, especially when cured under a hot humid (Mediterranean) climate. The results suggest the viability of application of such industrial waste products in concrete which, among others, is likely to have an important impact on waste utilisation strategy and a dual benefit of reducing the possible negative environmental impact and preservation of natural resources.

Key words: Ground granulated blastfurnace slag (GGBS), hot humid curing, hydration potential/products, Mediterranean environment, electric arc furnace steel slag, thermogravimetric analysis, X-ray diffraction analysis.

INTRODUCTION

Ferrous slags may be divided into two broad classes: those arising from the smelting of ores and those formed during refining of iron into steel. The former is mainly blast furnace slag, which is produced in very large tonnage in many developed countries as a by-product of the manufacture of iron in a blastfurnace. It results from the fusion of limestone flux with ash from coke and the siliceous and aluminous residue remaining after the reduction and separation of the iron from the ore. The production of iron and slag in a blastfurnace involves a continuous, rather than batch process, with both materials being produced in molten, homogeneous states. Much of the iron and steel slag produced around the world are slowly air-cooled, leading to the formation of a crystalline product. However, if the molten slag is cooled rapidly, for example by quenching with water, a granular glassy material is produced. This material, if collected, dried and ground to sufficient fineness is known to have latent hydraulic properties. It has been established that the main products of slag hydration is essentially the same as the principal product formed when PC hydrates (Mutasar, 2001; Neville, 1995) that is, calcium silicate hydrate (C-S-H). The main factors known to influence the hydraulic activity of slag cement include chemical composition, glass content, and fineness, activator content, curing temperature and water/cementitious material ratio (ACI Committee Report, 1987). GGBS has been used for decades as partial replacement material in concrete and has well established standards describing their use (ACI committee report, 1987; Concrete Society, 1991; Sersale et al., 1996).

*Corresponding author. E-mail:s.nwaubani@anglia.ac.uk.

Steel slag is formed when refining iron into steel in a conversion furnace. This is a batch process in which reactions are not always completed, thus resulting in a non-uniform slag that could still contain substantial amounts of free calcium and/or magnesium oxide (Caijun Shi, 2004). A more modern process involves the use of Electric-Arc Furnace such as that used by the Libyan Iron and Steel Company, hereafter referred to as LLS. The Electric-Arc furnace is able to produce very precise alloys when compared to the older Bessemer and Open-heart techniques. According to the technical bulletin produced by the Libyan Iron and Steel Company (1998), the company produces sponge iron by the direct reduction of iron ore with locally produced natural gas. This sponge iron is subsequently converted into steel in an Electric-Arc furnace, which uses an electric arc to heat the raw materials. In addition to the sponge iron, several other materials are added which includes; steel scrap, fluorspar, limestone and dolomite. The end product of the oxidation process is steel plus large quantities of slag. This type of steel slag is known to have similar composition with Portland clinker, having significant quantity of C_2S and C_3S (George, and Sorrentino, 1990). This waste material is traditionally utilised for road bases and as aggregates in concrete production in many countries (Manso et al., 2006). Its use as cement replacement material has also been established; however this is limited by a general lack of understanding of its hydration process and by its heterogeneity, coarseness and higher particulate density (Monshi and Asgarani, 1999; Moosberg-Bustnes, 2004).

This study looks at how the above factors influence the hydration properties of the two types of slag-cement mixtures investigated.

MATERIALS AND METHODS

Three cementitious materials were used in this study; Ordinary Portland cement (OPC), Ground Granulated Blast Furnace Slag (GGBS) and Air-Cooled Electric-Arc Furnace Steel Slag produced in Libya (LSS). The cement used was standard Portland cement conforming to harmonised British Standard Institution EN 197-1:2000. The GGBS used was supplied by the Blue Circle Group in the UK and conformed to the same harmonised standard. No such specification exists for the use of steel slag yet. The water used was clean distilled water.

Physical characteristics

The physical characteristics of the cementitious materials tested were: colour, relative density, specific surface area, the amorphous (glass) content and particle size distribution. The colour of the materials were evaluated visually and noted. The specific gravity, specific surface areas and the oxide compositions of the Portland cement and GGBS were supplied by the manufacturers but that for LSS was done in a commercial testing company. The LSS was ground in a Ball mill to a fineness powder and the particle size distribution of each of the three materials was then obtained by laser diffraction method using a Beckman-Coulter LS-230 apparatus, with a 750 nm laser beam capable of measuring particles as small as 0.04 µm. The physical characteristic of the materials used are shown in Table 1 and Figure 1.

Table 1. Physical properties of the cementitious materials.

Property	OPC	GGBS	LSS
Colour	Grey	White	Dark Grey
Relative density (g/cc)	3.181	3.025	3.617
Specific surface area (m^2/kg)	985	1571	1358
Glass content (%)	-	98	57

Chemical and mineralogical characteristics

It is well known that the X-Ray diffraction pattern for a crystalline substance can be considered to be a fingerprint, as each crystalline material has a unique diffraction pattern. From the diffraction pattern a semi-quantitative assessment of the crystallinity can be made and, by reference to standard patterns, the crystalline phases present can be identified. In this study, X-Ray diffraction technique was employed for identification of the mineralogical compound composition of the starting materials using a Philips (PW 1050/70) series automatic diffractometer with the following conditions and settings: 45 kV, 25 mA, Cu-Kα radiation, 0.1° 2θ step size, at 1 degree/minutes. The analysis covered the range 5- 60° 2θ. Figure 2, 3 and 4 show the respective X-Ray patterns for the un-reacted OPC, GGBS and the LSS powders used in this study.

Experimental mix proportions

To provide a sound basis for comparison of performance, all tests were carried out using paste mixes made with a constant water-cementitious material ratio of 0.4. A simple approach has been adopted which involves the replacement of 30% of the OPC used in the 100% OPC control samples (Mix O), with an equal weight of GGBS (Mix 30 G) or LSS (Mix 30 L).

Curing regimes

After mixing the paste, each mix was cast into glass bottles (approximately 15 mm diameter by 40 mm high). The bottles were then sealed with a snap-on plastic cap, covered with wet paper towel and placed in sealed plastic bags. The first set of samples were left to cure in the fog room maintained at an approximate temperature of 20 ± 2°C and 100% relative humidity (curing regime A) until tested. The second set of samples were cured in a room maintained at a constant temperature of 35 ± 2°C and approximate relative humidity of 70% RH (curing regime B), to replicate a Mediterranean climate(hot dry environments).

At the end of the specified curing period, the paste samples were subjected to a combination of TG and XRD analysis to ascertain the rate and extent of reactivity as well as the hydration products formed.

Thermogravimetric studies (TG)

Thermogravimetric analysis involves measuring the dynamic weight loss from a sample as it is heated at a controlled rate. It is a widely used quantitative technique in evaluating the hydration products of

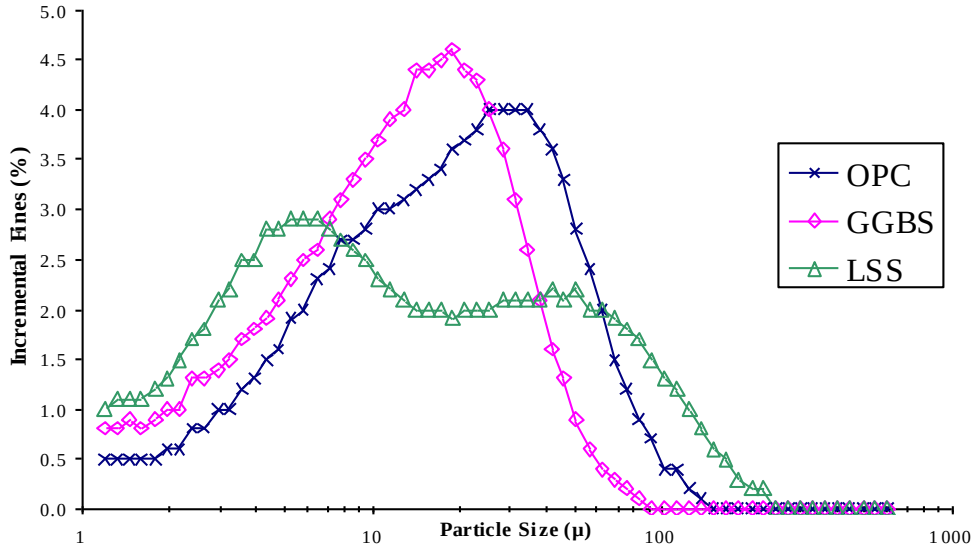

Figure 1. Particle size distribution of the cementitious materials.

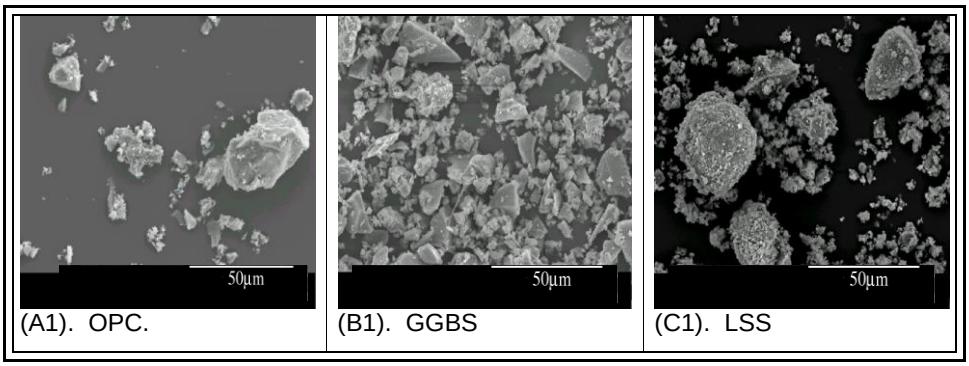

Figure 2. SEM images of the particles of the starting materials at 1K magnifications.

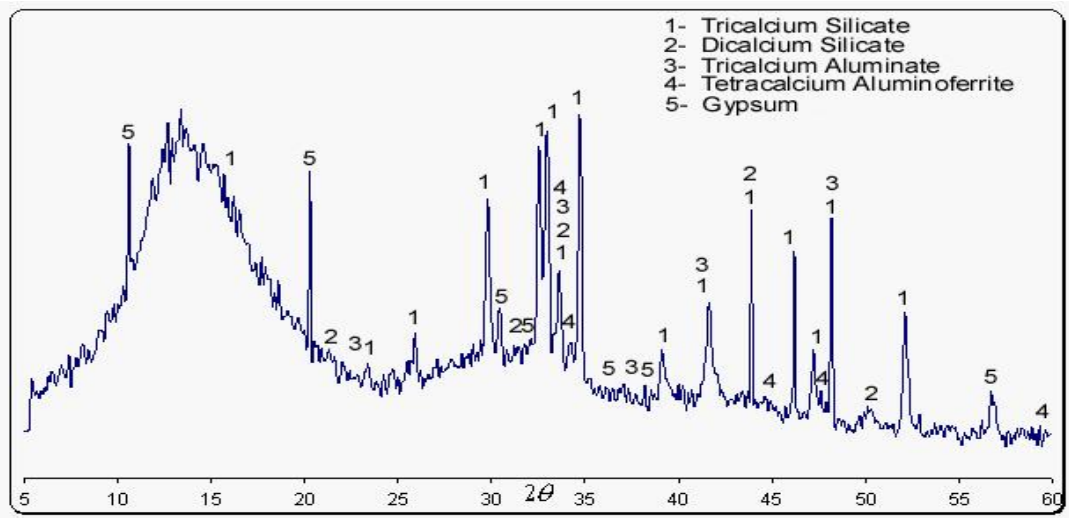

Figure 3. Mineralogical composition of un-reacted OPC.

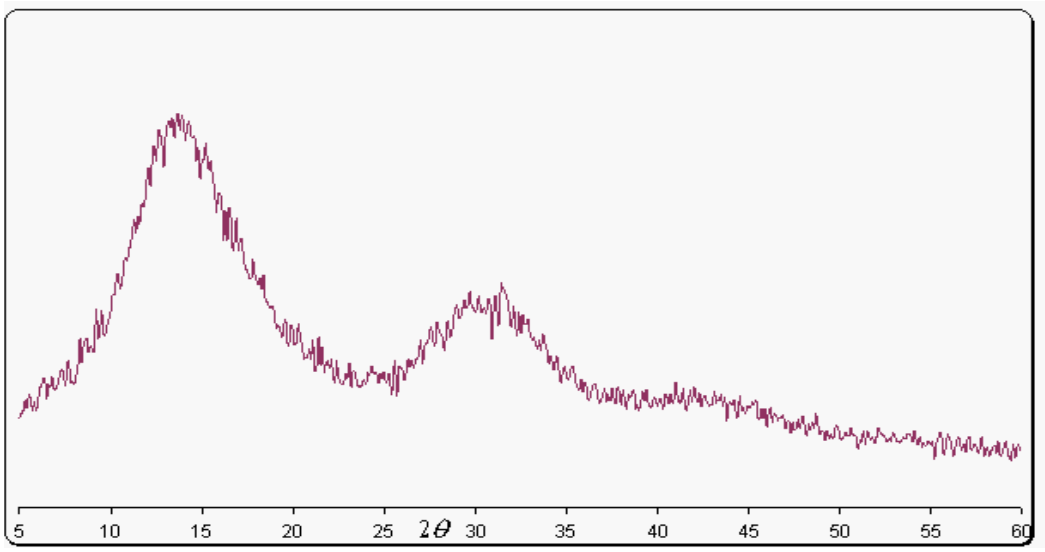

Figure 4. XRD trace of un-reacted GGBS.

cement pastes. This technique is based on the assumption that chemical reactions or decomposition of a given material usually occur within a fixed temperature range. Volatiles such as water of hydroxylation or crystallization, or gasses are given off resulting in weight change of the test sample. This enables quantitative identification of the minerals or compounds known to decompose within defined temperature ranges.

For cements, the weight loss in the temperature range of 425 to 550°C is due primarily to decomposition of calcium hydroxide (CH) or [$Ca(OH)_2$], and the peak of the temperature weight-loss curve, probably affords the best available method for determining this phase (Nwaubani, 1990). The loss below the CH step is due to the decomposition of Calcium Silicate Hydrate (C-S-H) and Calcium Aluminate Hydrate (C-A-H) phases. The weight loss above 550°C is partially due to CO_2 and partly due to the final stages of dehydration of C-S-H and the hydrated aluminate phases. Therefore, the degree of hydration may be assessed as a function of the amount of products decomposed in the temperature range from 100 to 425°C or by considering the amount of calcium hydroxide present in the system (Taylor, 1997).

In this investigation, only the weight loss in the temperature range of 100 to 425°C was used. The weight changes were measured using a Stanton Redcroft STA-1500 Balance. This involved heating test samples of about 30 mg from 25 to 1000°C at a constant heating rate of 20°C per minute in a dynamic Nitrogen atmosphere. The apparatus used was equipped with a programmer unit and connected to a computer and plotter for handling and analysis of the data as well as for outputting the TG results.

X-ray diffraction and scanning electron microscope studies

After curing in the respective regimes (for 12 h, 7 days, 28 days and 360 days), the specimens were dried at 60°C to constant weight. Then representative samples were taken from the inside of each specimen (free of carbonation), and prepared for the test by carefully crushing and sieving to pass a 45 µm sieve. The presence and relative quantities of the hydration products present in each sample was then evaluated using the X-Ray patterns obtained using standard X-Ray diffraction techniques performed on the Philips automatic diffractometer described above.

Scanning electron microscopy (SEM)

Powdered samples prepared as described above were coated with a film of gold and a Philip SEM 505 scanning electron microscope was used to obtain the micro-structural morphology of the hydration phases present.

RESULTS AND DISCUSSION

Physical characteristics of the starting materials

The physical characteristics of the starting materials are shown in Table 1. It shows that the relative density of the GGBS used was slightly less than that of OPC, whereas LSS has a much greater density value due to the high iron present in LSS as impurities (Table 2). The effect of incorporating LSS in a mix as an equal mass replacement for OPC is therefore likely to cause a significant decrease in the total volume of the cementitious powder. This decrease will result in a reduced volume of cement paste and an increased water-cementitious ratio on a volume basis, and consequently can be expected to affect the properties of the fresh and hardened mixes. Furthermore, GGBS has a glass content of 98%, whereas, LSS has a relatively low glass content, 57%, which is less than the 67% required by BS 6699: 1992 (specification for GGBS for use with Portland cement). The specific surface area (SSA) of LSS falls between that of GGBS and OPC. However, the particle-size distribution (Figure1) clearly shows that LSS is a much coarser material. It has a greater proportion of particles larger than 102 µm (6.2%) when compared to OPC (1.2%) and GGBS (0.1%). Such variation in particle-size constitutes a major determining factor of the reactivity potential of the cementitious materials used in

Table 2. Oxide chemical composition of the cementitious materials.

Compound	OPC (%)	GGBS (%)	LSS (%)
Silica (SiO_2)	20.31	35.61	16.76
Alumina (Al_2O_3)	5.04	12.21	6.11
Lime (CaO)	64.84	40.21	37.76
Ferric Oxide (Fe_2O_3)	2.74	0.80	19.51
Magnesia (MgO)	1.02	8.80	14.31
Potash (K_2O)	0.68	0.46	<0.01
Soda (Na_2O)	0.11	0.16	0.16
Titania (TiO_2)	0.28	0.55	0.93
Phosphorus Pentoxide (P_2O_5)	0.11	<0.02	0.47
Chromium Sesquioxide (Cr_2O_3)	0.21	<0.01	0.10
Manganese Oxide (Mn_2O_3)	0.07	0.46	2.45
Zirconia (ZrO_2)	<0.02	0.03	0.04
Hafnia (HfO_2)	<0.01	<0.01	<0.01
Lead Monoxide (PbO)	<0.02	<0.02	<0.02
Zinc Oxide (ZnO)	0.01	<0.01	<0.01
Barium Oxide (BaO)	0.02	0.11	0.05
Strontia (SrO)	0.16	0.08	0.02
Stannic Oxide (SnO_2)	<0.01	<0.01	<0.01
Cupric Oxide (CuO)	<0.01	<0.01	<0.01
Loss on Ignition at 1025^oC	1.30	1.07	0.53
Total	96.81	98.41	99.20

this study. The variation in particle sizes for the cementitious materials can also be seen in the Scanning Electron Micrographs shown in Figure 2.

Chemical characteristics of starting materials

The chemical oxide composition of the cementitious materials is presented in Table 2. The data show that the main components in OPC, GGBS and LSS are similar. However, there are variations in the proportions of these components. LSS has very high iron oxide content, 19.51%, when compared to 2.74 and 0.80% for OPC and GGBS respectively. The high iron content is a typical characteristic of steel slags and is one of the main reasons why they are not commonly used as cement replacement materials (Moosberg-Bustnes et al., 2004). However, this property is advantageous in situations where weight is a critical factor, as in foundations, shoring walls, noise barriers, insulations against radiation, etc. The amount of CaO + MgO + SiO_2, by mass, in LSS was found to be 68.83% which is marginally higher than the 66.66%, specified in BS 6699: 1992. Furthermore, the LSS contains CaO in similar proportions to those in GGBS but it is low in SiO_2 and high in MgO. It is also worth noting that the alkalinity factor ($CaO/SiO_2 + P_2O_5$) was found to be 2.19 in the LSS studied. This is greater than the 1.8 minimum specified by Wu et al. (1999) in order for steel slag to be used as a cement replacement material.

The XRD traces for these materials are presented in Figures 3, 4 and 5 respectively. The main crystalline compounds identified in the OPC (Figure 3), were tricalcium silicate (C_3S) or Ca_3SiO_5, dicalcium silicate Ca_2SiO_5 or (C_2S), tricalcium aluminate, tetracalcium aluminoferrite (C_4AF) and gypsum. The GGBS used was highly amorphous (approximately 98% glass content, Table 1), making it impossible to identify individual compounds using this method as shown in Figure 4. The LSS was more crystalline than the GGBS (approximately 57% glass content, Table 1), hence the XRD peaks were easier to identify as shown in Figure 5. It was possible to identify peaks consistent with the presence of tricalcium silicate (C_3S), dicalcium silicate (C_2S), magnesium oxide (MgO), iron oxide (Fe_2O_3), and tricalcium aluminate (C_3A). However, other peaks were present that could not be identified by reference to standard diffraction patterns. This is not unexpected as the LSS composition and structure is significantly different from that of OPC and GGBS. The high iron and magnesium contents are clearly evident.

TG analysis of the hydrated samples

A typical set of TG results is presented in Figure 6 as a function of the weight change per degree rise in temperature from 100 to 550°C. The total weight loss in this temperature range for the various mixes is summarized in Table 3 and in Figure 7 as a percentage of the original (dry) weight of the samples. The weight losses, excludes the decomposition of CH and are therefore due to the main hydration products formed, such as CH, C-S-H and C-A-H. The results show an increase in the measured weight loss with increasing age, suggesting progressive hydration with time. The influence of the curing regimes are clearly evident, therefore the results are discussed in the context of the two curing regimes used.

Influence of curing regime A

The results in Table 3 and Figure 7 show that the replacement of 30% of the OPC with GGBS or LSS led to a reduction in the amount of C-S-H and C-A-H produced during the first 12 h when compared with the OPC control mix. At 28 days, the GGBS blend produced similar quantities of C-S-H and C-A-H as the 100% OPC control mix but the LSS blend produced less. However, at 180 days mixes 30 G and 30 L produced more hydration products than the control mix.

The low reactivity of GGBS at early ages is well documented in the literatures (Taylor, 1997). However, with increasing curing time, the reactivity of the GGBS

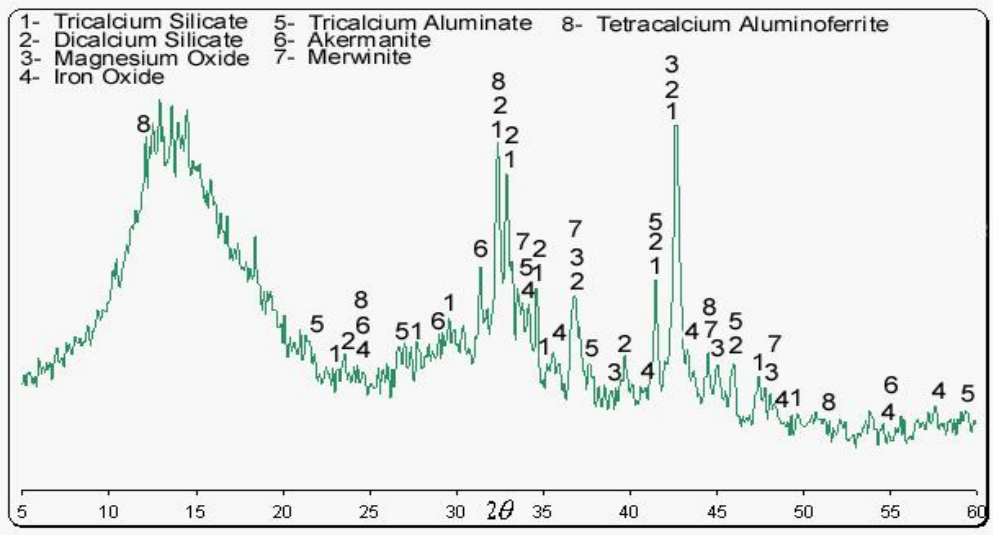

Figure 5. Mineralogical composition of un-reacted LSS.

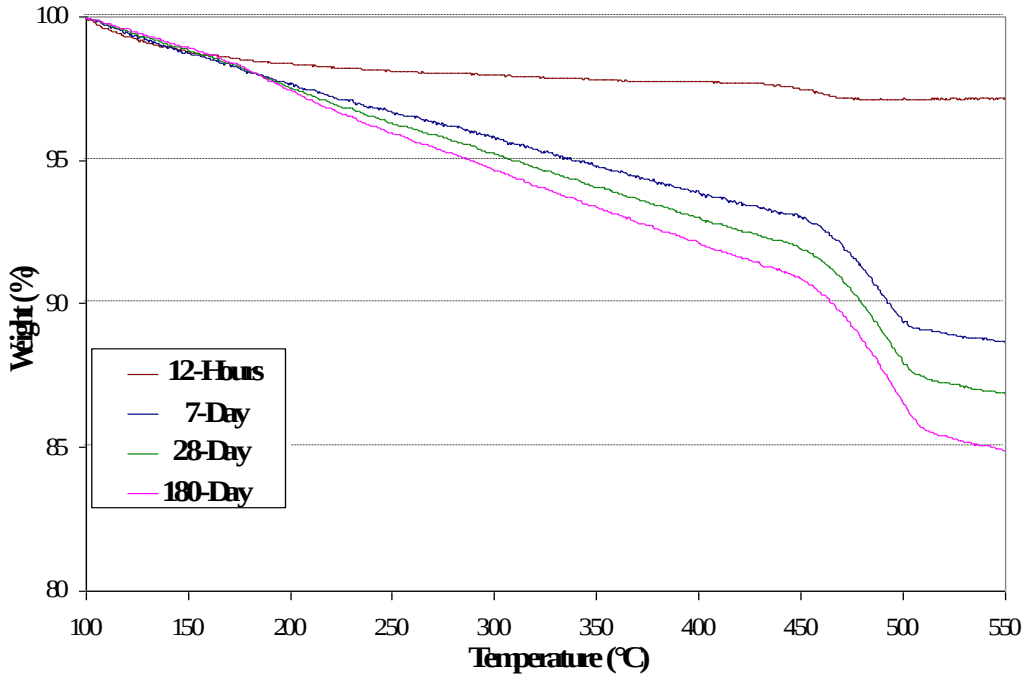

Figure 6. Typical TG curves for Mix O (100% OPC) cured under regime A.

Table 3. Total weight loss (%) between 100°C and 425°C for Mix O, 30 G and 30 L when cured under regime A or B.

Age	Total weight loss (%) for mixes cured under regime A or B					
	Mix O		Mix 30 G		Mix 30 L	
	Regime A	Regime B	Regime A	Regime B	Regime A	Regime B
12 h	2.40	3.06	1.35	2.81	1.20	1.81
7 days	7.84	7.59	7.91	8.74	7.11	7.54
28 days	8.63	8.02	8.72	9.35	7.99	8.21
180 days	8.84	8.64	10.27	10.59	9.03	9.09

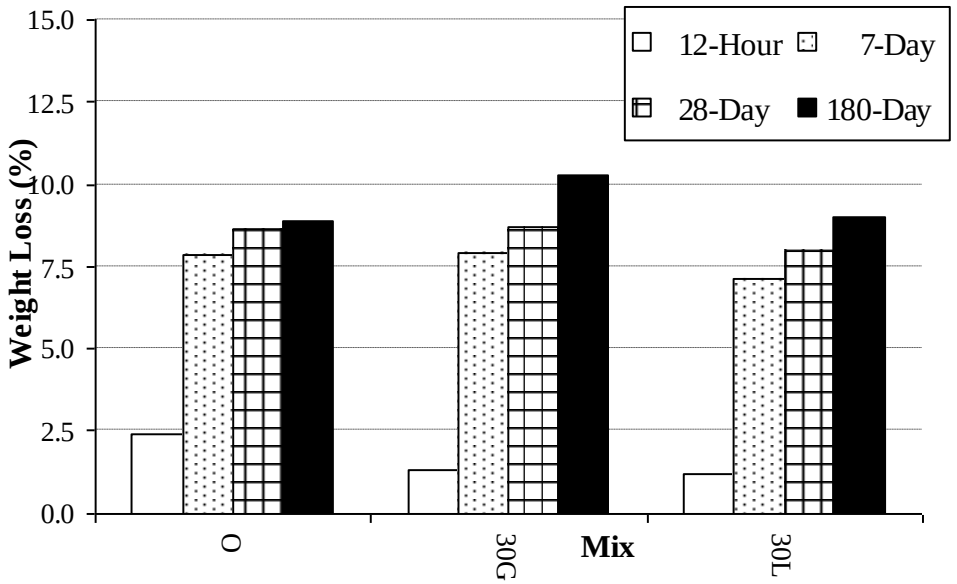

Figure 7. Total weight loss (%) between 100°C and 425°C for samples cured under regime A.

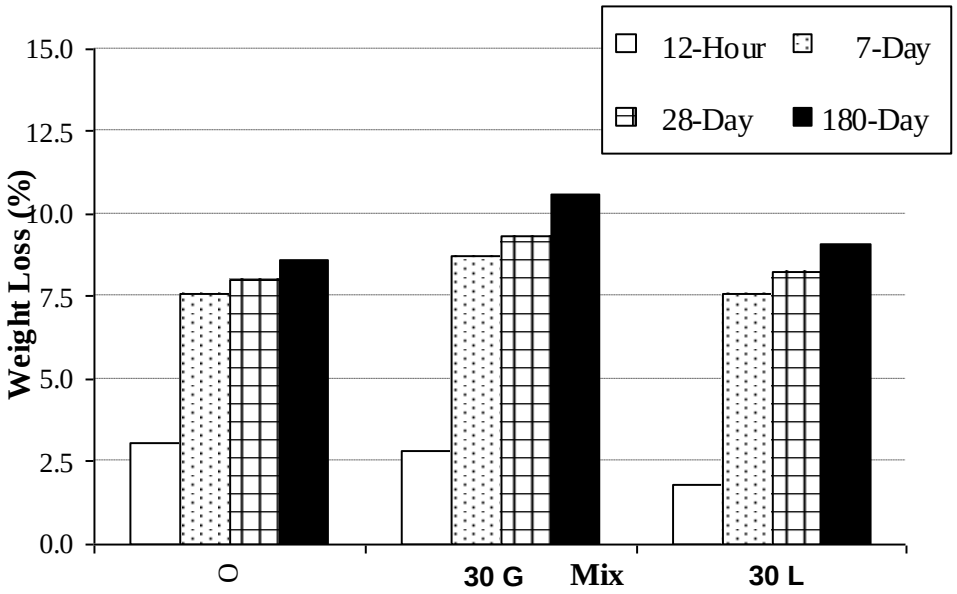

Figure 8. Total weight loss (%) between 100°C and 425°C for samples cured under regime B.

particles tends to increase leading to the formation of a greater volume of hydration products in the long-term. The increase in reactivity of GGBS is due to its activation by the alkalis released from the hydration of the OPC (ACI Committee Report, 1987; Taylor, 1997). Although the reactivity of the LSS particles seems to be following a similar trend to those of the GGBS, the variation in the amount of hydration products formed indicates that the LSS particles are less reactive than those of the GGBS (Muntasser, 2001) - Figures 7 and 8 as well as Table 3. This may be due to the lower glass content (57%, Table 1) and the presence of relatively large particles of the LSS (Figures 1 and 2) compared with glass content of 98% for GGBS (Table 1).

Influence of curing regime B

Figure 8 and Table 3 compare the weight losses in the temperature range of 100 to 425°C for Mix O, 30 G and

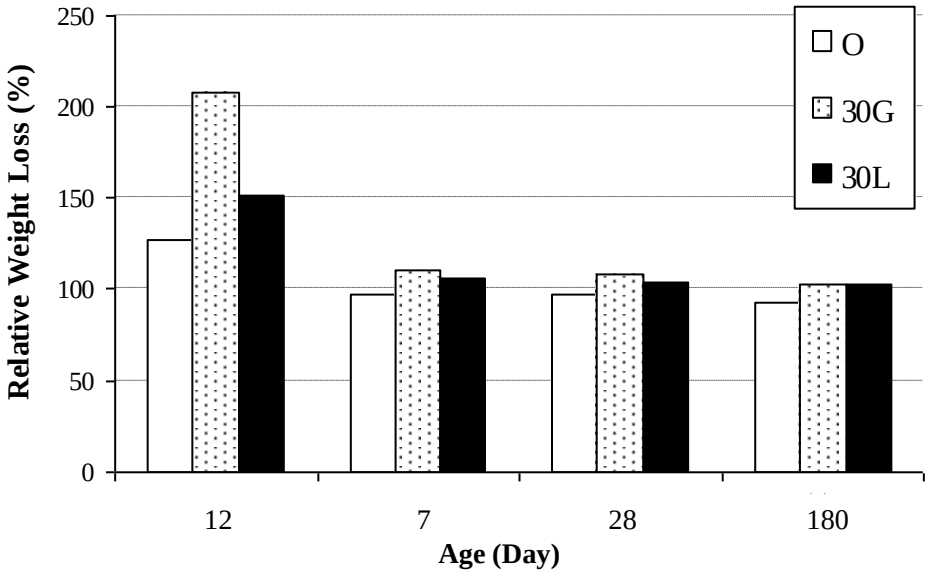

Figure 9. Relative weight loss (%) between 100 and 425°C when samples cured under regime B as compared to when cured under regime A.

30 L, when cured under regime B. The results show that, with respect to product formation, all mixes followed a similar trend to that observed when cured under regime A. However, differences exist when the intensities of the hydration product peaks are compared for the two different curing regimes.

Figure 9 shows the relative amount of hydration products formed by Mixes O, 30 G and 30 L in the two curing regimes. It can be seen that the amount of hydration products formed in mixes containing 30% GGBS or LSS were always greater when cured under regime B as compared to the corresponding mixes cured under regime A. This increase was most noticeable at early ages (before 12 h). These results suggest that mixes containing 30% GGBS or LSS favour curing under regime B. This is an important finding which may have far reaching implications when these materials are utilised for construction in hot-humid environments.

Relative weight loss (%) between 100 and 425°C when samples cured under regime B as compared to when cured under regime A.

$$\left(\frac{Weight\ loss\ at\ regime\ B}{Weight\ loss\ at\ regime\ A}\times 100\right)$$

XRD study of the hydrated samples

Figure 10 presents the XRD traces for Mix O, which is typical for all the other mixes investigated. They show that the addition of GGBS or LSS reduced the over-all XRD signal levels from the crystalline products. This reduction was more pronounced for mixes containing GGBS and may be due to the high amorphous (poor crystalline) nature of the hydration products formed. Significantly, this underlines the fact that the hydration properties of these mixes could not be investigated using XRD alone hence the use of thermogravimetry as a complementary technique.

The main crystalline compounds identified using XRD analysis were calcium hydroxide (CH), ettringite (calcium sulphoaluminate, $C_6A\overline{S}_3H_{32}$), calcite and calcium aluminate hydrate (C_4AH_{13} and C_3AH_6). It was also possible to identify peaks consistent with the presence of tricalcium silicates (C_3S), dicalcium silicates (C_2S), tetracalcium aluminoferrite (C_4AF) and gypsum at 12 hours. The presence of C_3S, C_2S, C_4AF and gypsum at 12 hours indicates that some un-reacted OPC was present. This is unsurprising since only about 70 and 30% of C_3S and C_2S typically reacts by 28 days respectively (Taylor, 1997). Figure 10 also shows that the height of the peaks associated with the presence of un-reacted compounds (peaks 6 to 10) in the OPC decreases with age whilst the CH peaks (peak 1) generally increases with age. The disappearance of the un-reacted compounds and the increase in CH is evidence that the cement particles continued to hydrate with age.

Conclusions

A summary of the main findings from this work are as follows:

1. Electric arc blast furnace Steel slag is clearly capable

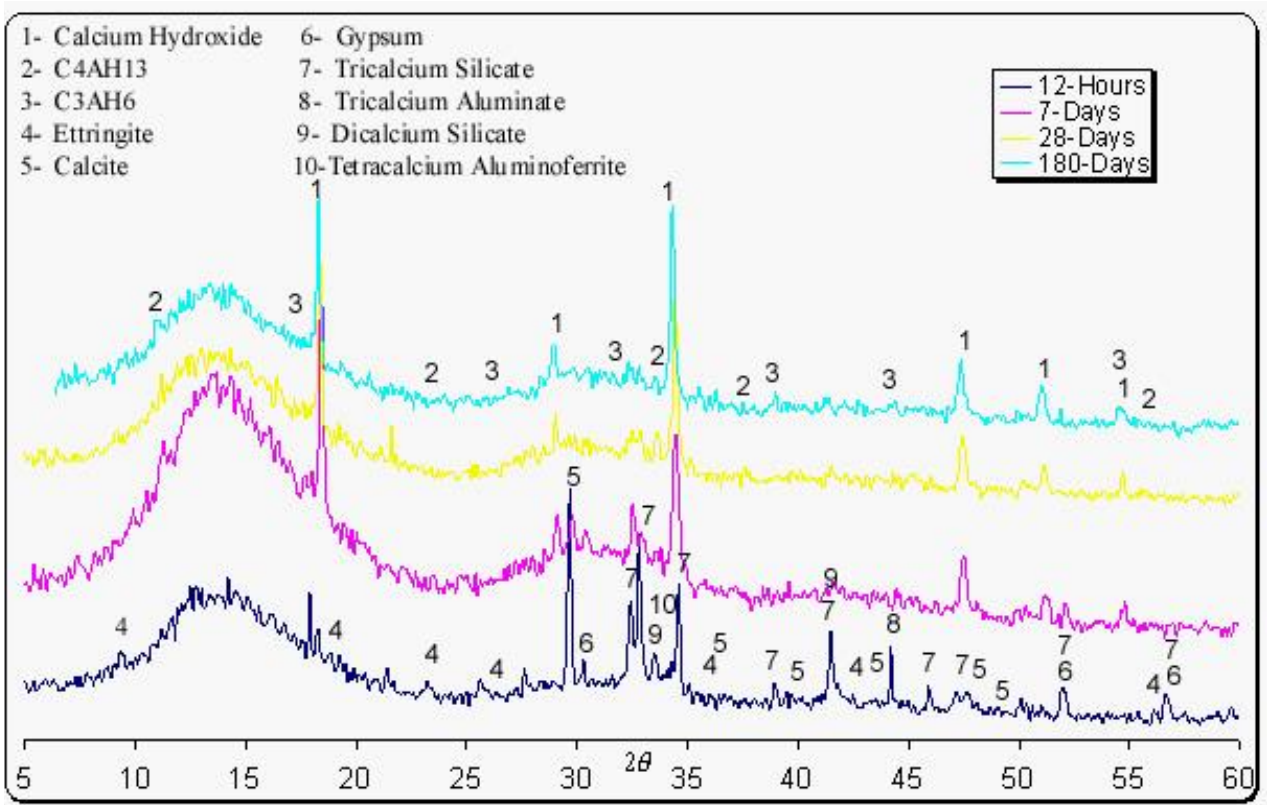

Figure 10. A typical XRD traces for 100% OPC control paste mixes when cured under regime A.

of reacting to form hydration products at normal temperatures.

2. The hydration of the LSS particles seems to follow a similar trend to that of the GGBS. However, the smaller weight loss values recorded for the OPC-LSS pastes suggests that the LSS particles were less reactive than those of the GGBS, This is most probably due to the low glass content and the presence of relatively larger but less amorphous particles in the LSS.

3. At early ages, the weight loss recorded for the OPC-GGBS paste was lower than that of the OPC. However, the cumulative weight loss of the former increased with prolonged curing period, leading to the formation of a greater volume of hydration products.

4. The hydration of the different cement pastes progressed at different rates. The rate and extent of hydration change when GGBS or LSS was used as OPC replacement.

5. Curing at elevated temperature seemed to increase the initial hydration rate of all the three mixtures studied but the relative weight loss are similar for all samples after curing for 28 days. No significant change or difference could be observed after 28 days.

6. From the point of view of hydration, mixes containing 30% GGBS or LSS responded better to curing under regime B, whereas the 100% OPC control mix favoured curing under regime A. This indicates a greater benefit of pozzolanic reaction in curing regime B and could have far reaching implications when binary mixtures incorporating slag are utilised for construction in hot-humid environments.

REFERENCES

ACI Committee 266 1R-87 (1987). “Ground granulated blast-furnace slag as a cementitious constituent in concrete”.

British Standard Institution, BS EN 197-1:(2000). “Cement-Part 1: Composition, specifications and conformity criteria for common cements”.

Caijun S (2004). “Steel Slag - Its production, processing, characteristics and cementitious properties”. J. Mater. Civ. Eng. 16(3):230–236.

Concrete Society (1991). “The use of GGBS and PFA in concrete”. Techn. Rep. 40:142.

George CM, Sorrentino FP (1990). “Valorization of basic oxygen steel slags”. International Congress on the Chemistry of Cements”. Paris, Theme 7(2):46-50.

Libyan Iron and Steel Company (1998). “Technical specification of products”. Quality Control Department, Musrata, Libya.

Manso JM, Polanco JA, Losañez M, Gonzalez JJ (2006). “Durability of concrete made with EAF slag aggregates”. Cem. Concr. Compos. 28:528–534.

Monshi A, Asgarani MK (1999). “Producing Portland cement from iron and steel slags and limestone”. Cem. Concr. Res. 29:1373-1377.

Moosberg-Bustnes H, Lind L, Forrssberg E (2004). “Fine particulate metallurgical by-products: An initial study of the influence on hydration and strength development”. Scand. J. Metall. 33(1):15-21.

Muntasser T (2001). “Properties and durability of slag based cement in the Mediterranean environment”. PhD Thesis, Department of Civil Engineering. University of Surrey.

Neville AM (1995). “Properties of Concrete”, Fourth Edition, Longman.
Nwaubani SO (1990). “Properties, durability and microstructure of pozzolanic concrete”. PhD Thesis, Department of Civil Engineering, University of Leeds.
Sersale R, Amicarelli V, Frigione G, Ubbriaco P (1996). “A study on the utilisation of an Italian Steel Slag”. Concresso Internacional de Quimica Do Cimento, 8. Rio de Janeiro. Commun. Theme 1(2):194-198.
Taylor HFW (1997). “Cement chemistry” second edition, Thomas Telford, UK.
Wu X, Zhu H, Hou X, Li H (1999). “Study on steel slag and fly ash composite Portland cement”. Cem. Concr. Res. 29:1103-1106.